Dynamic Article Links ▶

PAPER

Thermodynamic stability, structural and electrical characterization of mixed ionic and electronic conductor $La_2Mo_2O_{8.96}$

Jesús E. Vega-Castillo,[a,b] Uday K. Ravella,[c] Gwenaël Corbel,[c] Philippe Lacorre[c] and Alberto Caneiro*[a,b,d]

Thermogravimetric analysis (TGA) technique in controlled oxygen partial pressure (pO_2) atmospheres has been used to obtain equilibrium oxygen content data as a function of pO_2 on the $La_2Mo_2O_{9-\delta}$ system resulting from the partial reduction of fast oxide-ion conductor $La_2Mo_2O_9$ (LM). Thermodynamic conditions for stabilization of crystalline $La_7Mo_7O_{30}$ and amorphous $La_2Mo_2O_{7-y}$ at 718 °C have been determined and discussed. At 608 °C, the compound reported for the first time $La_2Mo_2O_{8.96}$ (LM896) has been found. The crystalline form and transition temperature in LM896 have been identified by X-ray diffraction at room temperature (XRD) and at controlled temperature. Conductivity curves obtained by electrochemical impedance spectroscopy (EIS) as a function of temperature for both LM and LM896 have been compared. The results indicate that LM896 is a mixed ionic and electronic conductor (MIEC).

Introduction

Solid oxide fuel cells (SOFC) use three basic components: a dense oxide ion conductor electrolyte, and two porous hybrid (cermet) or mixed ionic and electronic conducting electrodes, a cathode for oxygen reduction and an anode for fuel oxidation.[1,2] The currently used material as electrolyte in SOFCs is yttria stabilized zirconia (YSZ), which exhibits good ionic conductivity values only above 800 °C. This high temperature makes necessary the use of expensive interconnection materials such as lanthanum chromites. The decrease of operating temperature in SOFCs by at least 200 °C would lead to make this technology, known as intermediate temperature solid oxide fuel cells (IT-SOFC), economically competitive. $La_2Mo_2O_9$ (LM) is a fast oxide ion conductor discovered in 2000.[3] Above ∼580 °C this material undergoes a reversible α (monoclinic) to β (cubic) phase transition with an abrupt increase of ionic conductivity up to values about one order of magnitude higher than those of YSZ. The main drawback in order to implement LM as an electrolyte for IT-SOFC is its poor stability under reducing atmospheres at temperatures above 600 °C.[4,5] The family of oxide ion conductors obtained by cationic substitutions on LM, $La_{2-x}A_xMo_{2-y}B_yO_{9-\delta}$, is known as LAMOX.[6–19] The partial substitution of Mo by W, $La_2Mo_{2-y}W_yO_9$, has been reported to improve the stability of LAMOX compounds against reduction.[9,17,18]

The partial reduction of LM can lead to amorphization or to the formation of phases with different crystalline structures and oxygen contents. Different authors have found an amorphous phase after partially reducing LM under diluted hydrogen at temperatures from 600 to 760 °C.[9,18,19] This amorphous compound presents electronic conductivity and it has been tested as sulfur tolerant anode material for SOFC.[24] The stabilization of perovskite related $La_7Mo_7O_{30}$ at temperatures between 700 and 760 °C in reducing atmosphere has also been observed.[18,19] In a previous work we have found that at 1000 °C, the reduction of LM results into the apparition of a mixture of two partially reduced molybdate phases, whose compositions depend on the oxygen partial pressure (pO_2) range.[5]

Some works suggest that LM can keep its crystal structure under certain reductive conditions and even behave as mixed ionic and electronic conductor (MIEC). Georges *et al.* reported the conservation of LAMOX structure after reducing LM in Ar–(10%)H_2 at 605 °C.[21] Marrero-López *et al.* also found by X-ray diffraction (XRD) that LM keeps its structure after annealing in Ar–(5%)H_2 at temperatures below 700 °C for 24 h.[22] These results are in apparent contradiction with a more recent work,[5] in which a continuous reduction of LM ceramic is detected at 608 °C under Ar–(10%)H_2, leading to amorphization. This discrepancy could be attributed to the dependence of the reduction path in LM on the gas flow rate which is relatively high, 6 L h^{-1}, in the last cited work.[5] Indeed, Jacquens *et al.* performed electrochemical impedance spectroscopy (EIS) measurements on $La_2Mo_{2-y}W_yO_9$ annealed in Ar–(10%)H_2 flowing at 0.6 L h^{-1} at 608 °C.[25] After annealing for 24 h at 608 °C, all cubic W-LAMOX specimens, even the most sensitive member of this series, $\alpha La_2Mo_2O_9$, have kept their initial structure. The increase in total conductivity measured in dilute hydrogen is ascribed to

[a]Instituto Balseiro, Centro Atómico Bariloche, 8400 San Carlos de Bariloche, Río Negro, Argentina
[b]Consejo Nacional de Investigaciones Científicas y Técnicas CONICET, Argentina
[c]LUNAM Université, Université du Maine, CNRS UMR 6283, Institut des Molécules et des Matériaux du Mans, Avenue Olivier Messiaen, 72085 Le Mans Cedex 9, France
[d]Comisión Nacional de Energía Atómica CNEA, Argentina. E-mail: caneiro@cab.cnea.gov.ar

the generation of an electronic contribution arising from the partial reduction of molybdenum. This contribution is more pronounced when the temperature and the tungsten content y are low.

Recently, Goel *et al.* analysed the increase of electrical conductivity on $La_2Mo_{2-y}W_yO_9$ under Ar–(10%)H_2.[26] They found that the electrical conductivity of these partial reduced samples varies depending on both the porosity of initial ceramics and the W content.

In this work, we aim to analyse the stability limits of pO_2 for LM at equilibrium conditions and temperatures close to those meant for IT-SOFC operation. We also study the ranges of stability of the phases present in the $La_2Mo_2O_{9-\delta}$ system at these temperatures.

Experimental

Synthesis of LM powders and ceramics

$La_2Mo_2O_9$ raw powders were prepared by standard solid state reaction. Stoichiometric amounts of La_2O_3 and MoO_3 were weighed and mixed in an agate mortar. La_2O_3 was previously dehydrated and decarbonated at 1000 °C for 2 h. The mixed oxides were annealed at 500 °C for 12 h to prevent Mo sublimation and then fired at 900 °C for 12 h. Several grindings and heat treatments were necessary to obtain pure LM.

In order to prepare a dense LM pellet, 5 g of raw powders were ball-milled into an agate jar with 20 agate balls (10 mm in diameter) in ethanol for 15 min. Approximately 500 mg of milled powder were shaped into a cylindrical pellet by pressing uniaxially under 1 ton. The green pellet was sintered at 1200 °C for 2 h. The sintered pellet had 92% of the theoretical density value with thickness and diameter of 4.53 and 5.30 mm, respectively.

Equilibrium TGA and pO_2 control

Equilibrium measurements at constant temperatures of 718 and 608 °C in a controlled atmosphere were carried out by using a Cahn 1000 thermobalance coupled to an electrochemical pO_2 control system.[27] Atmospheres with controlled pO_2 are set by flowing a carrier gas through an electrochemical oxygen pump and an electrochemical oxygen sensor. The pump enables to modify the pO_2 in the gas following Faraday's law while the sensor uses Nernst's law to measure the set pO_2 value. The symmetrical thermobalance allows both to detect when the steady state is reached and to measure the oxygen content of the sample.

Ar, CO_2 and Ar–H_2 were used as carrier gases to supply the oxygen pump. The highest pO_2 corresponded to that obtained in Ar ($pO_2 = 3 \times 10^{-6}$ atm, value due to residual oxygen in commercial Ar 5.0). Intermediate pO_2 range was set by electrochemical reduction of CO_2 giving CO–CO_2 atmospheres. The low pO_2 implemented range was obtained by oxidizing Ar–H_2 and generating Ar–H_2–H_2O. The gas flow rate for all equilibrium measurements was set to 6 L h^{-1}. Each equilibrium point was recorded after a constant TGA signal (mass variation lower than 1 μg) for at least 5 h.

Approximately 500 mg of LM raw powder were placed into an alumina crucible in the thermobalance. The sample was

heated up in flowing Ar; once at the working temperature, the equilibrium was reached. The mass value obtained under Ar with $pO_2 = 3 \times 10^{-6}$ atm was used as reference for stoichiometric $La_2Mo_2O_9$ ($\delta = 0$). This reference was verified under pure oxygen ($pO_2 = 1$ atm). The pO_2 value was then decreased by switching the atmosphere and the annealing maintained until a new equilibrium was detected. This procedure was repeated as the pO_2 was gradually decreased down to the minimum adjustable value with dry Ar–H_2.

Structural characterization

The phase purity of powder and pellet samples after their annealing in the thermobalance and quenching under controlled oxygen partial pressure was checked by XRD at room temperature. Diffractograms were collected on a Philips PW1700 diffractometer with Cu($K_{\alpha 1} + K_{\alpha 2}$) radiation and a graphite monochromator and a PANalytical q/q Bragg-Brentano X'pert MPD PRO diffractometer Cu($K_{\alpha 1} + K_{\alpha 2}$) equipped with the X'Celerator multi-elements detector.

In situ XRD measurements under controlled oxygen partial pressure were carried out at different annealing temperatures by using an Anton-Paar HTK10 camera coupled to the electrochemical pO_2 control system described in the previous subsection. In this manner it is possible to record XRD patterns at high temperature under controlled pO_2 atmosphere.

Electrical characterization

LM and LM896 were characterized by EIS in different atmospheres using a symmetrical electrochemical cell. Pt electrodes were sputtered onto both flat sides of cylindrical LM pellet. The sample was placed in an alumina cell inside a cylindrical furnace, with Pt mesh as current collectors. This setup can also be connected to the electrochemical pO_2 control system.

EIS spectra were collected from 250 up to 608 °C by means of a frequency response analyser (FRA) coupled to an Autolab potentiostat, within a frequency range of 1 MHz to 0.1 Hz and voltage amplitude of 50 mV. The measured spectra were analyzed using Zview software.[28] A R||Cpe circuit was used to model the high frequency contribution (bulk) for spectra recorded in air and Ar (stoichiometric LM). For spectra recorded on partially reduced $La_2Mo_2O_{9-\delta}$, $0 < \delta \leq 0.04$, in Ar–H_2–H_2O atmosphere, the high frequency contribution was adjusted with only one resistance element. The total conductivity values σ for LM and $La_2Mo_2O_{9-\delta}$ were calculated from the resistance values R in the respective equivalent circuits, the measured thickness L and surface area A of the pellet as follows: $\sigma = L(AR)^{-1}$. For all spectra, the Pt electrode contribution was modelled with a short Warburg element in series with the high frequency circuit.

Results and discussion

Reduction of $La_2Mo_2O_9$ at 718 °C: stability of $La_7Mo_7O_{30}$ and amorphous $La_2Mo_2O_{7-y}$

The oxygen content $9 - \delta$ in $La_2Mo_2O_{9-\delta}$ as a function of decreasing pO_2 at 718 °C is shown in Fig. 1. As explained in Experimental section, the first measurement was performed in Ar (closed square) and afterwards the pO_2 was gradually

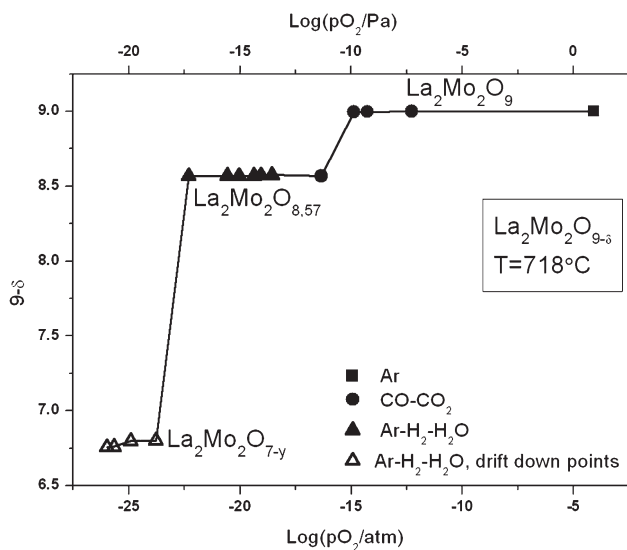**Fig. 1** Oxygen content as a function of pO_2 in $La_2Mo_2O_{9-\delta}$ at 718 °C.
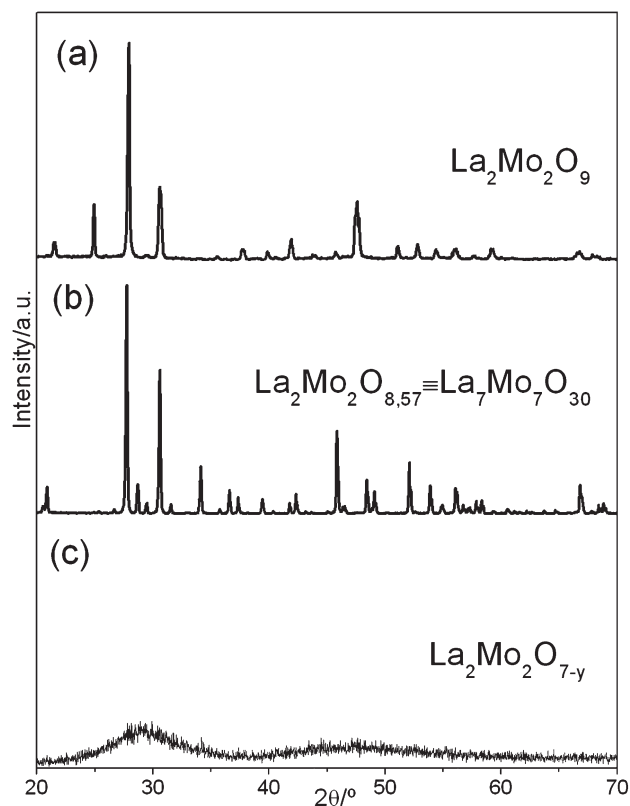

Fig. 2 XRD patterns of $La_2Mo_2O_{9-\delta}$ stabilized at 718 °C in different atmospheres and quenched down to room temperature with $9 - \delta$ values of (a) 9, (b) 8.57 and (c) $7 - y$.

decreased. The oxygen content remains as 9 as long as the pO_2 is above 10^{-15} atm. It delineates the thermodynamic stability range for stoichiometric LM at 718 °C. As pO_2 is slightly decreased down to 10^{-16} atm, an abrupt oxygen loss of $\delta = 0.43$ is observed after five days. A further decrease of the oxygen partial pressure down to 10^{-22} atm does not induce any change in the oxygen content of the sample. Therefore, the $9 - \delta = 8.57$ stoichiometry is thermodynamically stable at 718 °C within the range $10^{-22} < pO_2 < 10^{-15}$ atm.

When decreasing pO_2 below 10^{-22} atm a slow reduction takes place again and in this case a steady state, indicating thermodynamic equilibrium, is never properly reached. Instead, a pseudo-plateau with a drift down is detected in the TGA signal *vs.* time at $9 - \delta$ values lower than 7 (open triangles in Fig. 1). The presence of a linear drift that increases when pO_2 decreases suggests that the compound $La_2Mo_2O_{7-y}$ has no fixed oxygen stoichiometry and it losses oxygen continuously with kinetics depending on the pO_2.

In order to determine the nature of phases (or mixture of phases) corresponding to the found stoichiometries $9 - \delta = 8.57$ and $7 - y$, two batches of LM raw powders were annealed at 718 °C in the TGA equipment in atmospheres with pO_2 values of 10^{-20} and 10^{-24} atm, respectively. Once the oxygen content of each batch reached constant 8.57 and $7 - y$ (with a drift as described in previous paragraph), respectively, the samples were quenched down to room temperature while maintaining the atmosphere. XRD patterns of quenched powders compared to those of initial LM are shown in Fig. 2. $La_2Mo_2O_{8.57}$ has been confirmed as $La_7Mo_7O_{30}$ perovskite related phase, while $La_2Mo_2O_{7-y}$ is amorphous.

Discussion on equilibrium pO_2 data at 718 °C

Several authors have observed the formation of $La_7Mo_7O_{30}$ as intermediate product during partial reduction of LM in different reducing atmospheres.[18,19] Indeed, Goutenoire was able to synthesize a large amount of $La_7Mo_7O_{30}$ in order to determine its crystal structure from neutron diffraction analysis by reducing LM in N_2–(6%)H_2 at 760 °C.[23] Nevertheless, they clarify that if

the atmosphere and temperature are maintained the reduction continues until amorphization of the compound. In other words, $La_7Mo_7O_{30}$ is a meta-stable phase at 760 °C in N_2–(6%)H_2 atmosphere. We think that the reproducible transient stabilization of $La_7Mo_7O_{30}$ from reduction of LM in N_2–(6%)H_2 at 760 °C is due to kinetic effects related to the gas flow rate (not specified in the cited work) and also to the used gas mixture. In fact, we have been able to reproduce Goutenoire's experiment under the same conditions obtaining the TGA plateau of $La_7Mo_7O_{30}$. Nevertheless when we have repeated the experiment under the same conditions but replacing N_2–(6%)H_2 by Ar–(5%)H_2, this plateau was not reached and the reduction continued directly until the amorphization of the sample.

In our equilibrium experiments, $La_7Mo_7O_{30}$ remained stable at 718 °C in atmospheres with pO_2 values within the range $10^{-22} < pO_2 < 10^{-15}$ atm (we have kept the treatment for even several days with no change observed in the mass signal). This indicates that $La_7Mo_7O_{30}$ is thermodynamically stable in the described conditions. The use of high gas flow rates in our equilibrium experiments enhances the kinetics of the reduction processes and avoids confusing meta-stable states with thermodynamically stable ones.

Regarding the observed amorphous compound (see Fig. 2(c)), in our previous work we had referred it to $La_2Mo_2O_{6.88}$.[5] Nevertheless, subsequent experiments including the one here reported indicate an oxygen non-stoichiometric range for this amorphous phase, leading us to revise that chemical formula. We have opted to use $La_2Mo_2O_{7-y}$ as approximated chemical formula for this

amorphous material. We deduce from our measurements that y in $La_2Mo_2O_{7-y}$ should be in the $0 < y < 1$ range.

Reduction of $La_2Mo_2O_9$ at 608 °C: stability and characterization of $La_2Mo_2O_{8.96}$

In order to determine whether the $La_7Mo_7O_{30}$ phase exists at a lower temperature, an equilibrium experiment in controlled atmosphere at 608 °C was performed.

Fig. 3 shows the oxygen content $9 - \delta$ in $La_2Mo_2O_{9-\delta}$ as a function of pO_2 at 608 °C. At this temperature the pO_2 stability limit for $La_2Mo_2O_9$ is 10^{-22} atm. Below this value the sample undergoes a slight reduction down to an oxygen content of 8.96. The stoichiometry 8.96 remains unchanged within the range $10^{-25} < pO_2 < 10^{-23}$ atm. Below 10^{-25} atm the sample reduces slowly down to amorphous $La_2Mo_2O_{7-y}$.

The reproducibility of $La_2Mo_2O_{8.96}$ (LM896) was checked by several oxidizing–reducing cycles between $9 - \delta = 9$ and 8.96. LM896 can also be recovered by oxidation from amorphous $La_2Mo_2O_{7-y}$. The reproducibility of LM896 upon reduction–oxidation confirms that the found pO_2 values corresponding to LM896 represent true thermodynamic equilibrium states. LM896 powders for XRD characterization were obtained from annealing LM at 608 °C in an atmosphere with a pO_2 of 10^{-24} atm in the TGA setup until total stabilization at $9 - \delta = 8.96$ was reached. The reduction of 500 mg from LM to LM896 took 200 min. The homogeneously light gray LM896 powders were then quenched down to room temperature and analyzed by XRD; the results are shown in Fig. 4. The X-ray diffractograms of LM and LM896 are identical. Both pseudo-cubic (2 3 1) reflections (at 2θ around 47.5°) are compared in the inset, the notorious peak splitting characteristic of $\alpha La_2Mo_2O_9$ indicates that LM896 has also a monoclinic symmetry at room temperature. XRD patterns of LM and quenched LM896 were fitted using constant scale factors (Lebail) within FULLPROF software,[29] in monoclinic $P2_1$ space group ignoring weak ($2 \times 3 \times 4$) superstructure peaks.[30] The obtained cell volumes were 366.05(1) Å^3 for LM and 365.71(1) Å^3 for LM896 showing a slight contraction after reduction. The respective cell parameters were $a = 7.1414(1)$ Å, $b = 7.1538(1)$ Å, $c = 7.1653(1)$ Å and $\beta = 89.530(1)°$ for LM and $a = 7.1411(1)$ Å, $b = 7.1520(1)$ Å, $c = 7.1608(1)$ Å and $\beta = 89.584(1)°$ for LM896.

The structure of $\alpha La_2Mo_2O_9$ has been described as one of the most complex structures reported to date.[31] The monoclinic cell has a number of formula units $Z = 48$, so, the chemical formula contained in the asymmetric cell can be written as $La_{96}Mo_{96}O_{432}$. In the case of $\alpha La_2Mo_2O_{8.96}$, 48 formula units would equal to $La_{96}Mo_{96}O_{430}$. This corresponds to a loss of two O atoms per monoclinic cell, which is consistent with maintaining the monoclinic $P2_1$ symmetry of $\alpha La_2Mo_2O_{8.96}$, with departure from $La_2Mo_2O_9$ of 2 equivalent O atoms related by the 2_1 screw axis.

HT-XRD on LM896 powders

In order to determine if LM896 undergoes a monoclinic–cubic transition, approximately 20 mg of LM raw powders were heated up to 608 °C inside the HT-XRD setup in He atmosphere. At this temperature, the atmosphere was switched to He–Ar–H$_2$–H$_2$O with a set pO_2 of 10^{-24} atm. After 200 min of annealing,
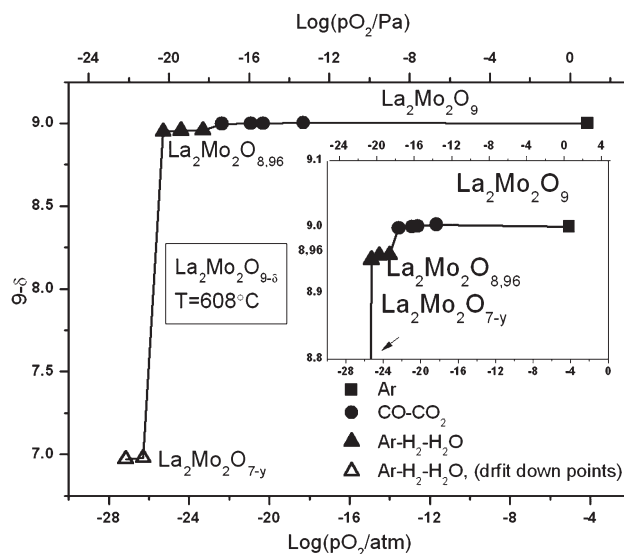
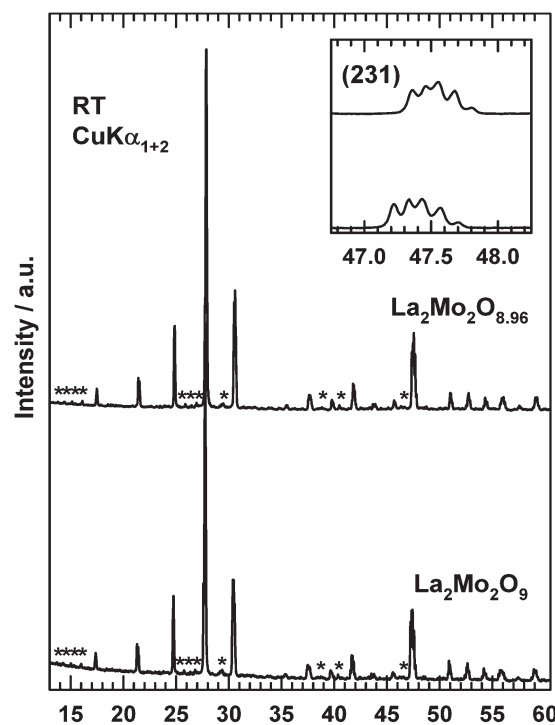**Fig. 3** Oxygen content as a function of pO_2 in $La_2Mo_2O_{9-\delta}$ at 608 °C.

Fig. 4 Room-temperature X-ray diffraction patterns of raw $La_2Mo_2O_9$ and quenched $La_2Mo_2O_{8.96}$ powder samples showing the superstructure peaks (*) and the splitting of the cubic (2 3 1) peak (inset), both characteristic of the monoclinic low temperature α form.

the stabilization of $La_2Mo_2O_{8.96}$ was assumed, based on the kinetics observed in TGA experiments described in previous subsection. Fig. 5 shows the XRD pattern collected at 608 °C on the LM896 phase (black line) in the vicinity of the most intense (1 2 0) peak of a beta-LM-type phase (gray line). A slight shift to higher 2θ values is visible indicating once again a contraction of the unit cell after reduction from LM to LM896. At 608 °C LM896 is in cubic symmetry (isostructural to $\beta La_2Mo_2O_9$) as indicated by the absence of splitting in (2 3 1) reflection shown
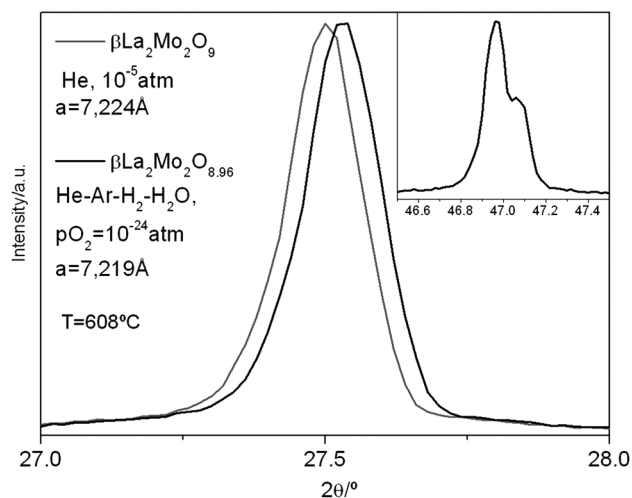
Fig. 5 Comparison of XRD patterns at 608 °C of cubic LM and LM896: main, (1 2 0) reflection and in the inset, (2 3 1) reflection for LM896 at 608 °C.
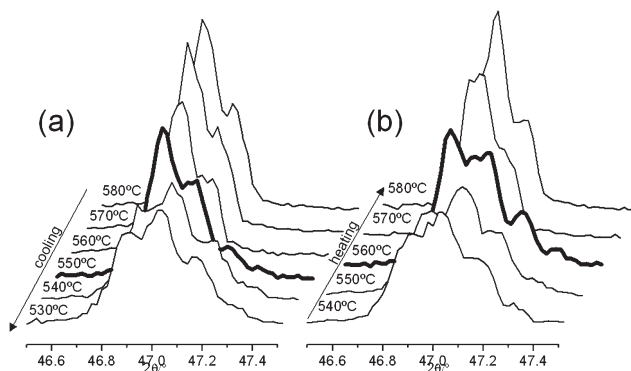

Fig. 6 Cubic or pseudo-cubic (2 3 1) XRD reflection for LM896 at different temperatures: (a) while cooling down, (b) while heating.

in the inset of Fig. 5 (double reflection due to CuK$_{\alpha1}$ and CuK$_{\alpha2}$ radiations). The cubic cell parameters obtained from Rietveld refinement in $P2_13$ space group are 7.2240(1) Å for LM and 7.2195(1) Å for LM896.

Aiming at determining the $\alpha \leftrightarrow \beta$ transition temperature for LM896, the (2 3 1) reflection was monitored at different temperatures by HT-XRD while cooling down from 608 °C. Fig. 6 shows how the monoclinic distortion shows up at 550 °C upon cooling, while on heating, both symmetries coexist at 560 °C. These values are identical to those observed for LM powders in air upon both cooling and heating in the same HTXRD setup.

Electrical characterization of La$_2$Mo$_2$O$_{8.96}$

As other authors have observed, the partial reduction of Mo in La$_2$Mo$_2$O$_{9-\delta}$ leads to an increase of electrical conductivity.[20,25,26] This behaviour would be expected for LM896 compound. Arrhenius plots of measured conductivity values for both LM (in air) and LM896 (in Ar–H$_2$–H$_2$O) are shown in Fig. 7. The curve corresponding to LM (squares) was recorded while heating up to 608 °C in air. At this point the atmosphere was switched by Ar–H$_2$–H$_2$O with a controlled pO_2 of 10^{-24} atm. The total resistance of the sample was then monitored as a

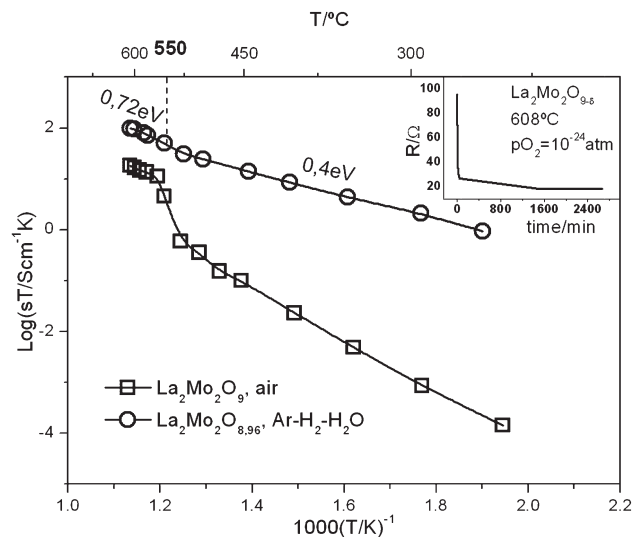**Fig. 7** Conductivity as a function of temperature for LM in air and LM896 in Ar–H$_2$–H$_2$O.

function of time (see inset in Fig. 7) and once a plateau was obtained, the stabilization of LM896 was assumed, after 40 h. The Arrhenius curve of LM896 shows a significant increase of conductivity values compared to those of LM, for instance at ~500 °C the difference is about two orders of magnitude. The curve presents two visible linear zones with different slopes with a break at around 550 °C. From adjusting the linear zones with Arrhenius's law, the calculated activation energies are 0.4 and 0.72 eV for the low and high temperature zones, respectively. Keeping in mind that 550 °C is the measured $\beta \rightarrow \alpha$ transition temperature for LM896 at cooling, the increase of activation energy can be related to the increase of ionic conductivity associated to this transition. The implemented technique does not allow to discriminate between electronic and ionic conductivity components. Nevertheless, the low activation energies for LM896 suggest predominant electronic conductivity.

Discussion on La$_2$Mo$_2$O$_{8.96}$

Some authors have suggested that LM exhibits both ionic and electronic conductivities while being partially reduced at temperatures close to 600 °C.[22,25] In fact, Jacquens et al. reduced a LM pellet in Ar–(10%)H$_2$ at 608 °C while monitoring its conductivity by EIS. Once they found stabilization of resistivity values, they characterized the conductivity of the reduced sample as a function of temperature while cooling down in the same atmosphere.[25] The results obtained by Jacquens et al. are identical to those reported in this work on La$_2$Mo$_2$O$_{8.96}$ electrical characterization. In the cited work, after EIS experiments, XRD identification showed the conservation of LAMOX structure so the authors concluded that LM can withstand partial reduction without decomposing.

We suspect that the results of Jacquens et al. correspond to MIEC La$_2$Mo$_2$O$_{8.96}$ and they were able to stabilize this compound in dry Ar–(10%)H$_2$. This is in apparent contradiction with our equilibrium results, in which while decreasing the pO_2 down to 20^{-26} atm, the compound amorphizes. Theoretically, the oxygen activity in pure dry Ar–H$_2$ should tend to zero (log pO_2

$\rightarrow -\infty$). Nevertheless, in the practice, there is always residual oxygen in high purity gas mixtures and there are leakages in any gas circuit. The effect of incoming oxygen through leakages is more important when the flow rate of the gas source is low since the total flux is the arithmetical addition of all individual gas inputs. Jacquens *et al.* used a very low flow rate (0.6 L h^{-1}) of dry Ar–(10%)H$_2$ so only a small amount of incoming air could have been enough to oxidize a part of H$_2$ setting an Ar–H$_2$–H$_2$O atmosphere. One of the aims of using high gas flow rate (6 L h^{-1}) in our experiments is to minimize the effect of the leakages in controlled atmospheres. Another one is to minimize oxygen pressure gradient around the sample by flushing it out.

The high oxide ion conductivity of βLa$_2$Mo$_2$O$_9$ has been attributed to its crystalline structure and explained with a lone-pair substitution concept.[32] Since the cationic framework of the LAMOX structure is seemingly preserved after reduction, it suggests that oxide ions remain mobile in La$_2$Mo$_2$O$_{8.96}$. On the other hand, the EIS measurements show considerably higher total conductivity values with low activation energies for LM896 compared with those of LM at temperatures below 608 °C. These facts lead us to conclude that the difference in conductivity values between LM and LM896 is due to the appearance of significant electronic conductivity in the latter compound. LM896 is an MIEC stable in reducing atmospheres. Thermal and chemical compatibilities of LM896 with LAMOX based electrolyte materials are presumed, with this novel MIEC being part of the LAMOX family as well.

The compensation of charges for La$_2$Mo$_2$O$_{8.96}$, assuming that the valence state for La and O are 3+ and 2− respectively, yields a total valence state of +5.96 for Mo. The reduction of Mo^{6+} to Mo^{6+}/(4%)Mo^{5+} combination is therefore compensated by the generation of O vacancies. The reduction to LM896 takes place at 608 °C in cubic beta form; this structure has three oxygen sites and two of those, O2 and O3, are partially occupied. It is logical to suppose that oxygen leaves from O2 and/or O3 sites. In the alpha form there are 216 oxygen sites and the vacancies might have a statistical distribution in several sites. Nevertheless, the strict plateau reached at $9 - \delta = 8.96$ leads us to think that the vacancies should correspond to a full loss at one monoclinic site. Unfortunately, the information available from the present study is not enough to clarify the oxygen vacancies distribution in LM896, neither in alpha or beta symmetry.

The decrease of the unit cell volume indicates that the slight decrease in oxygen stoichiometry involves a larger reduction in volume than the expansion arising from the increase in ionic radius as the valence state of molybdenum is lowered (0.455 Å for Mo^{6+} and 0.497 Å for Mo^{5+} in 4.5 coordination). Note that in β-LM, taking into account the partial occupancy of O2 and O3 sites, the average number of oxygen atoms surrounding Mo is 4.5.

Conclusions

The thermodynamic pO$_2$ limits for LM at 718 and 608 °C were determined as 10^{-15} and 10^{-22} atm, respectively. The stability range for perovskite related compound La$_7$Mo$_7$O$_{30}$ at 718 °C was found between 10^{-15} and 10^{-22} atm of pO$_2$. The novel compound La$_2$Mo$_2$O$_{8.96}$ was found at 608 °C within the range of $10^{-23} < p$O$_2 < 10^{-25}$ atm. This material is isostructural to α(monoclinic) La$_2$Mo$_2$O$_9$ below 560 °C and undergoes a

transition to a β(cubic) LAMOX structure above this temperature. LM896 is a mixed conductor that exhibits an important electronic conductivity component added to the ionic conductivity values of LM oxide conductor.

References

1 A. Lashtabeg and S. J. Skinner, *J. Mater. Chem.*, 2006, **16**, 3161.
2 O. Yamamoto, *Electrochim. Acta*, 2000, **45**, 2423–2435.
3 P. Lacorre, F. Goutenoire, O. Bohnke, R. Retoux and Y. Laligant, *Nature*, 2000, **404**, 856–8.
4 D. Marrero-López, J. C. Ruiz-Morales, D. Pérez-Coll, P. Núñez, J. C. C. Abrantes and J. R. Frade, *J. Solid State Electrochem.*, 2004, **8**, 638–643.
5 J. Vega-Castillo, L. Mogni, G. Corbel, P. Lacorre and A. Caneiro, *Int. J. Hydrogen Energy*, 2010, **35**, 5890–5894.
6 C. Tealdi, G. Chiodelli, L. Malavasi and G. Flor, *J. Mater. Chem.*, 2004, **14**, 3553.
7 X. Wang, Z. Cheng and Q. Fang, *Solid State Ionics*, 2005, **176**, 761–765.
8 D. Marrero-López, D. Perez-Coll, J. C. Ruiz-Morales, J. Canales-Vázquez, M. C. Martín-Sedeno and P. Nunez, *Electrochim. Acta*, 2007, **52**, 5219.
9 X. P. Wang, Q. F. Fang, Z. S. Li, G. G. Zhang and Z. G. Yi, *Appl. Phys. Lett.*, 2002, **81**, 3434.
10 A. Subramania, T. Saradha and S. Muzhumathi, *J. Power Sources*, 2007, **167**, 319.
11 S. Georges, F. Goutenoire, F. Altorfer, D. Sheptyakov, F. Fauth, E. Suard and P. Lacorre, *Solid State Ionics*, 2003, **161**, 231.
12 D. Marrero-López, J. Canales-Vázquez, W. Zhou, J. T. S. Irvine and P. Núñez, *J. Solid State Chem.*, 2006, **179**, 278–288.
13 G. Corbel, P. Durand and P. Lacorre, *J. Solid State Chem.*, 2009, **182**, 1009–1016.
14 D. Marrero-López, P. Núñez, M. Abril, V. Lavín, U. R. Rodríguez-Mendoza and V. D. Rodríguez, *J. Non-Cryst. Solids*, 2004, **345–346**, 377–381.
15 G. Corbel, E. Chevereau, S. Kodjikian and P. Lacorre, *Inorg. Chem.*, 2007, **46**, 6395–404.
16 S. Basu, P. S. Devi and H. S. Maiti, *J. Electrochem. Soc.*, 2005, **152**, 2143–2147.
17 Z. S. Khadasheva, N. U. Venskovskii, M. G. Safronenko, A. V. Mosunov, E. D. Politova and S. Y. Stefanovich, *Inorg. Mater.*, 2002, **38**, 1168–1171.
18 G. Corbel, Y. Laligant, F. Goutenoire, E. Suard and P. Lacorre, *Chem. Mater.*, 2005, **17**, 4678–4684.
19 J. A. Collado, M. A. G. Aranda, A. Cabeza and S. Bruque, *J. Solid State Chem.*, 2002, **85**, 80–85.
20 P. Pinet, J. Fouletier and S. Georges, *Mater. Res. Bull.*, 2007, **42**, 935–942.
21 S. Georges, F. Goutenoire, Y. Laligant and P. Lacorre, *J. Mater. Chem.*, 2003, **13**, 2317.
22 D. Marrero-López, J. Canales-Vázquez, J. Ruiz-Morales, J. Irvine and P. Núñez, *Electrochim. Acta*, 2005, **50**, 4385–4395.
23 F. Goutenoire, *J. Solid State Chem.*, 1999, **142**, 228–235.
24 X. C. Lu and J. H. Zhu, *J. Electrochem. Soc.*, 2008, **155**, B1053.
25 J. Jacquens, D. Farrusseng, S. Georges, J.-P. Viricelle, C. Gaudillère, G. Corbel and P. Lacorre, *Fuel Cells*, 2010, **10**, 433–439.
26 M. Goel, E. Djurado and S. Georges, *Solid State Ionics*, 2011, **204–205**, 97–103.
27 A. Caneiro, P. Bavdaz, J. Fouletier and J. P. Abriata, *Rev. Sci. Instrum.*, 1982, **53**, 1072.
28 Scribner Associates, ZView™, *A Software Program for IES Measurements and Analysis*, 2007.
29 J. Rodríguez-Carvajal, *Physica B: Condensed Matter.*, 1993, **192**, 55–69.
30 S. Georges, R. A. Rocha and E. Djurado, *J. Phys. Chem. C*, 2008, **112**, 3194–3202.
31 I. R. Evans, J. A. K. Howard and J. S. O. Evans, *Chem. Mater.*, 2005, **17**, 4074–4077.
32 P. Lacorre, *Solid State Sci.*, 2000, **2**, 755–758.